

The biocalcarenite stone of Agrigento (Italy): Preliminary investigations of compatible nanolime treatments

TAGLIERI, Giuliana, OTERO, Jorge, DANIELE, Valeria, GIOIA, Gianluca, MACERA, Ludovico, STARINIERI, Vincenzo <<http://orcid.org/0000-0002-7556-0702>> and CAROLA, Asuncion Elena

Available from Sheffield Hallam University Research Archive (SHURA) at:
<http://shura.shu.ac.uk/17566/>

This document is the author deposited version. You are advised to consult the publisher's version if you wish to cite from it.

Published version

TAGLIERI, Giuliana, OTERO, Jorge, DANIELE, Valeria, GIOIA, Gianluca, MACERA, Ludovico, STARINIERI, Vincenzo and CAROLA, Asuncion Elena (2018). The biocalcarenite stone of Agrigento (Italy): Preliminary investigations of compatible nanolime treatments. *Journal of Cultural Heritage*, 30.

Copyright and re-use policy

See <http://shura.shu.ac.uk/information.html>

The biocalcarenite stone of Agrigento (Italy): Preliminary investigations of compatible nanolime treatments

Giuliana Taglieri^a, Jorge Otero^b, Valeria Daniele^{a,*}, Gianluca Gioia^a, Ludovico Macera^a, Vincenzo Starinieri^b, Asuncion Elena Charola^c

^aDepartment of Industrial and Information Engineering and Economics, University of L'Aquila, via G. Gronchi 18, 67100 L'Aquila, Italy

^bMaterials and Engineering Research Institute, Sheffield Hallam University, S1 1WB Sheffield, UK

^cMuseum Conservation Institute, Smithsonian Institution, Washington, DC, USA

Abstract

Nanolime is a promising consolidant for the conservation of most historic structures thanks to its high compatibility with carbonate-based substrates. Nanolime can recover the superficial cohesion of deteriorated surfaces thanks to its potential to complete the carbonation process, recreating a thin network of new cementing calcium carbonate. In this paper, the nanolime was produced by an innovative, time and energy-saving and scalable method, and its efficacy was tested preliminarily on biocalcarenite stones from Agrigento. The stones characterization as well as the treatment effectiveness, in terms of protection against water and superficial consolidation, was investigated by several techniques such as X-ray fluorescence, X-ray diffraction, scotch tape test, water absorption by capillarity, mercury intrusion porosimetry, drilling resistance measurement system and colorimeter. Investigations showed that nanolime could guarantee a complete transformation in pure calcite together with a superficial consolidation and a reduction in water absorption.

1. Introduction

Calcareous materials have been one of the main construction materials throughout the ages and proved to be very durable over the centuries. However, they may suffer several degradation processes (e.g. flaking of the surface, powdering and formation of small blisters) that can be recovered through the application of consolidants. Over the last century, several consolidants have been used: silicate-based products or organic consolidants, such as alkoxysilanes, acrylic, epoxy or vinyl resins, have been commonly used in restoration treatments, mainly due to their immediate strength enhancement and ease of application. However, the low physico-chemical compatibility, the lack of bonding between the mineral calcareous matrix and the consolidant material and even the deterioration of the organic consolidant itself, discourages their use and in some cases may compromise the conservation of the monument [1–3]. Inorganic consolidants and, among others, lime-based consolidants present the great advantage of their total chemical compatibility with the calcitic substrate, thanks to their aptitude to react with atmospheric carbonic dioxide to produce calcium carbonate (carbonation process). However, traditional lime-based treatments were considered to have some limitations, such as the reduced impregnation depth and the very slow rate of carbonation [4–6]. In order to reduce such limitations, in 2001 Ca(OH)₂ nanoparticles, dispersed in an alcoholic or hydro-alcoholic medium, (nanolimes) were synthesised. So far, nanolimes have been tested on mural paintings, stuccoes and natural stones, and on all the carbonatic-based substrate where a restoration treatment was required [5,7–20]. The efficacy of nanolime dispersions can be affected by several factors, such as the dispersion concentration, solvent type, porosity of the substrates to be treated and relative humidity (RH) conditions. It is commonly agreed that lower concentration of the suspensions (i.e. 5 g/L) help reduce the accumulation of the consolidating product near the surface and significantly improve the yield of carbonation in the pores [16,17]. Furthermore, it has been proved that the concentration and the number of treatments cycles have a significant influence on the strengthening effect, in relation to the stone porosity as well [16,18]. A percentage of residual water content in the dispersing medium (> 10% in volume) clearly enhanced the carbonation process [19]. Recent investigations suggests that nanolime penetrates well in porous materials, but it can be transported back to the surface as the solvent evaporates [20]. Moreover, the type of alcoholic solvent and the RH conditions seem to have an influence on the rate of the carbonation reaction, and the formation of different polymorphs of calcium carbonate [21,22]. Currently, nanolimes have been synthesized according to several routes, [10,23–26], where Ca(OH)₂ was rarely the only reaction product. Washings and purification steps were frequently needed to eliminate the by-products and/or organic compounds, leading to low yield and prolonged synthesis time. The development of a versatile, cost effective and up-scalable method can be essential to the success of introducing nanolime for widespread usage on carbonatic substrates. Recently, an innovative and patented method, based on the ion exchange process, was proposed [27]. This method worked at room temperature and ambient pressure, and it allowed producing, in few minutes and without intermediate steps, pure and crystalline Ca(OH)₂ nanoparticles in aqueous suspension. The resulting portlandite nanocrystals, less than 100 nm in size, are very reactive, with a complete carbonation process, forming pure calcite in few hours or up to 7 days, depending on solvent, concentration and RH of the environment [28–31]. In addition, the produced nanolime can be dispersed, at different solid concentrations, in mixed water/alcohol (W/A) mixtures in order to improve both the colloidal stability and/or the amounts of consolidant. Specifically, nanolime dispersions in a mixture of 50% water and 50% iso-propanol in volume, (W/A = 50%), demonstrated to be particularly suitable in optimizing the carbonation process [14,29]. The aim of the present work is to test the effectiveness of this nanolime as a compatible treatment on biocalcarenite stones. Specifically, these stones constitute the building material used for most of the buildings of the “Valley

of the Temples” in Agrigento – Sicily, Italy, characterized by a documented advanced decay [32–34]. The paper has been divided into three parts:

- synthesis and characterization of the nanolime; · characterization of the biocalcarene stone from a physicochemical and mechanical point of view;

- testing, in a preliminary way, of different nanolime formulations by varying the solvents and the nanolime concentration. The evaluation of the treatment effectiveness in terms of protection against water and superficial consolidation was properly investigated.

2. Research aim

Colloidal $\text{Ca}(\text{OH})_2$ nanoparticles (also called nanolime) are emerging as effective conservation material for all carbonatic-based substrate. Nanolime can recover the superficial cohesion of deteriorated surfaces, thanks to its potential to complete the carbonation process, recreating a thin network of new cementing calcium carbonate. In the present paper we report, for the first time, results about the effectiveness of the treatments by a not commercial nanolime on biocalcarene stones from “Valle dei Templi” – Agrigento. In particular, the nanolime is synthesized in laboratory by our original, eco-friendly, one-step and scalable method that provides pure and crystalline nanoparticles in a reproducible way. Moreover, the simplicity and rapidity of this novel procedure provides an ideal opportunity to scale up the nanoparticles production in order to extend their uses in all the application fields where large amounts of such compatible consolidant should be requested. The effectiveness of the nanolime treatments, in terms of reduction of porosity, protection against water absorbed by capillarity and superficial consolidation, is investigated by means of several techniques. The physico-chemical and mechanical characterization of the untreated stones is reported too.

3. Material and methods

3.1. Synthesis and characterization of nanolime

$\text{Ca}(\text{OH})_2$ nanoparticles were synthesized by an anionic exchange process, at room temperature and ambient pressure, by mixing under moderate stirring an anion exchange resin with an aqueous calcium chloride solution [27]. The supernatant water of the produced nanolime suspension (NW) was partially extracted and substituted with isopropanol or with 1-butanol. Three nanolime dispersions were prepared: two of them, named $N_{50\%}$ and $N_{50\%}^*$, were characterized by a water/isopropanol mixture, ($W/A = 50\%$), and a solid concentration of 5 g/L and 10 g/L, respectively; and the third dispersion, named N_B , was characterized by a water/1-butanol mixture ($W/A = 5\%$) and a solid concentration of 5 g/L. In particular, N_B was considered to assess its influence on nanolime performance due to its slow evaporation rate. The size, shape and degree of agglomeration of the nanoparticles were determined by transmission electron microscopy (TEM, PhilipsCM200) and the crystalline phase was analyzed by XRD (PAN-alytical XPertPRO). Both TEM and XRD samples were prepared diluting the suspension in ethanol under nitrogen atmosphere to avoid the carbonation process. In addition, by means of XRD, we analyzed the carbonation reaction of each dispersion, taking 0.12 mL of nanolime sample, left to dry in air in room conditions ($T = 20 \pm 2^\circ\text{C}$, R.H. $\approx 50 \pm 5\%$), until complete solvent evaporation (about 20 minutes). XRD patterns were recorded in step size of $0.026^\circ 2\theta$, in the angular range $10\text{--}70^\circ 2\theta$. HighscorePlus software by PANalytical and ICSD and ICDD reference databases were used for the mineralogical identification and to perform the quantitative analysis (Rietveld refinement). Kinetic stability of the produced suspensions was determined by turbidity measurements, analysing their absorbance at $\lambda = 600\text{ nm}$ by using UV/VIS Spectrophotometer (Lambda 2 Perkin-Elmer). Before the test, nanolimes were sonicated for 20 minutes (Ultrasonic bath by Ultra Sonik 300) to reduce the nanoparticle agglomeration. Measurements were taken for up to 2 hours. The KS % was measured in function of time and was calculated using the following formula: $\text{KS \%} = 1 - [(A_0 - A_t)/A_0] \times 100$ where A_0 is the starting absorbance and A_t the absorbance at time t , both evaluated at wavelength 600 nm [35]. The relative kinetic stability (KS %) decreases as result of the nanoparticle settling; values range from 0 (unstable dispersion) to 100 (not settling of the nanoparticles).

3.2. The Agrigento’s biocalcarene

The stones used in this work, which were obtained from the local quarry of Villasetta, have similar characteristics to the ones used for the construction of the Temples [36]. Chemical, mineralogical and physical features of the stones were studied using different techniques. A general examination was performed using a stereomicroscope (SM, Leica Stereozoom S8APO). The chemical and mineralogical composition was determined by X-Ray Fluorescence (XRF, Philips PW2440), X-Ray Diffraction (XRD, PANalytical XPert PRO) and Attenuated Total Reflectance – Fourier Transform Infrared, (ATR-FTIR, Thermo Nicolet Nexus instrument). In particular, XRF samples were prepared as FP pellets. For XRD measurements, stone samples were milled and sieved through a $50\ \mu\text{m}$ mesh and placed over a XRD zero-background sample holder; the patterns analysis was performed as reported above. FTIR spectra were collected by 64 scans in the range $400\text{--}4000\text{ cm}^{-1}$ at a spectral resolution of 4 cm^{-1} . The obtained FTIR spectrum was identified using the Infrared and Raman users Group (IRUG) libraries, the HR Hummel Polymer and Additives library as well as the ASTER mineral library. The pore structure of the stone was determined, on three samples (named B_1 , B_2 and B_3 respectively), by Mercury Intrusion Porosimetry, (MIP, PASCAL 140/240). A contact angle of 141° was assumed between mercury and the stone. An equilibration time of 30 s was used between each pressure increase step and the measurement of the intruded volume. Prior to MIP analysis, samples were dried in a fan-assisted oven at 80°C to

constant weight. The water absorption by capillarity (WAC) of the stones was measured on three cubic samples ($30 \times 30 \times 30$ mm) following the standard procedure [10]. A Drilling Resistance Measurement System (DRMS) from SINT-Technology was used to measure changes in strength along the drilling path into the stone. The DRMS measures the force required to drill a hole at constant rotation (rpm) and lateral feed rate (mm/min). The force is known to correlate with the compressive strength of the material. Values were calculated as mean of 3 tests. The test was carried out using drill bits of 5 mm diameter, rotation speed of 200 rpm, a rate of penetration of 15 mm/min and penetration depth of 10 mm.

3.3. Nanolime treatments applied on the Agrigento stones

In order to investigate, in a preliminary way, the nanolime effectiveness in reducing capillary water absorption and yielding superficial consolidation, three stones samples with irregular shape, S1, S2 and S3 (Fig. 1a), were treated with $N_{50\%}$, $N^*_{50\%}$ and N_b respectively.

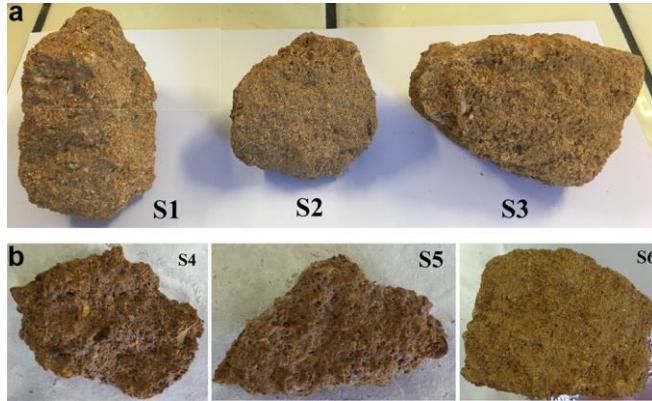


Figure 1 Irregular biocalcarene samples used for the nanolime treatments: a: S1 (approx. 17 cm^2), S2 (approx. 14 cm^2) and S3 (approx. 17 cm^2); b: S4 (approx. 13 cm^2), S5 (approx. 5 cm^2) and S6 (approx. 22 cm^2).

The use of irregularly shaped stone samples was considered to reproduce the real in situ application on irregular surfaces. Nanolimes were applied by brushing until stone saturation was achieved, by using about 100 mg of calcium hydroxide for each stone surface. Brushing treatment was applied to the side with largest and mostly flat surface (approx. 10 cm^2 each). Straight after treatment, samples were wiped with a wet cloth to remove the excess of consolidant and to mitigate surface whitening. Stones were stored for 2 days at $\text{RH} = (75 \pm 5)\%$. Then, the samples were oven-dried at 60°C until constant mass was reached, and then stored in a desiccator. Finally, we considered additional three samples (Fig. 1b): two for WAC (S4, S5 samples) and one (S6 sample) for the STT and DRMS resistance measures (carried out on 6 different points, in order to reduce the influence caused by the inhomogeneity of the stone). These were treated with nanolime applications repeated three times, following the same procedure reported above. In particular, for S4, S5 and S6 samples, we used the $N^*_{50\%}$ nanolime suspension that provided, as shown in the results section, the best compromise in terms of treatment efficacy and costs. The effectiveness of the treatments, in terms of protection against water and superficial consolidation, was evaluated by means of several tests. WAC was carried out, before and after treatment, following the method proposed by LNEC [37]. For each sample, we measured the values of the coefficient of average absorption in 30 minutes (CA), the amount of absorbed water at the end of the test (Qf) and the variation of CA values referred to untreated and treated stones (ΔCA). The effective protective efficacy (Ep), defined as the percentage variation of Qf before and after treatment, was evaluated too. Surface cohesion was estimated by the "Scotch Tape Test" (STT), according to ASTM D3359 [38]. Results were taken as the mean of three tests for each sample. In order to better assess the improvement of the consolidation efficacy of the treatment, we evaluated the difference of the superficial resistance (untreated and treated) using DRMS, generally considered the most suitable methodology for quantifying consolidation effectiveness and penetration depth of the consolidant, particularly in soft stones [39]. Pores size distribution and open porosity was measured by MIP; the tests were carried out on samples measuring approximately $8 \times 8 \times 8$ mm taken from both treated and untreated stones. Finally, the color changes, before and after treatment, were evaluated on samples S1, S2 and S3 by using a spectrophotometer (Minolta CM508D Colorimeter) in CIE-Lab system colorimeter [40], considering 10 evaluations per stone in different areas of the treated face. Total color variation (ΔE) was calculated by the formula:

$$\Delta E = \sqrt{\Delta L^*{}^2 + \Delta A^*{}^2 + \Delta B^*{}^2}$$

where ΔL^* was the change in luminosity (white-black parameter), Δa^* (red-green parameters) and Δb^* (blue-yellow parameters) were the chromaticity coordinates. Analyses were focused on total color variations and changes in the luminosity (white-black parameters).

4. Results and discussion

TEM micrograph on the nanolime sample NW (Fig. 2a) showed nanoparticles with dimensions < 20 nm, with a tendency to agglomerate forming hexagonally shaped clusters. XRD results revealed that only pure $\text{Ca}(\text{OH})_2$ was formed after synthesis (Fig. 2b).

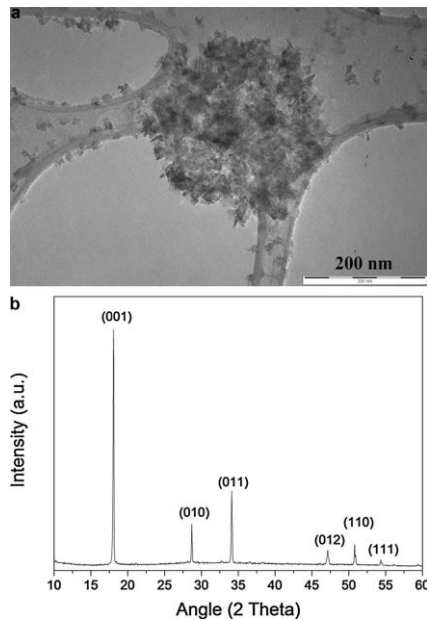


Figure 2 a: TEM micrograph of the nanolime sample Nw; **b:** XRD pattern of dried particles from Nw sample. Bragg peaks of $\text{Ca}(\text{OH})_2$ pattern (ICSD#96-100-8782) were indexed.

From the analysis of the carbonation process, we observed that whilst $\text{N}_{50\%}$ and $\text{N}_{50\%}^*$ showed a completed carbonation process, i.e., pure calcite (CaCO_3), only a partial conversion into calcite was observed for N_B (Fig. 3a). In addition, an intermediate and metastable form, namely calcium carbonate hydroxide hydrate (CCH), was observed as in previous work [29]. As concerns the kinetic stability (Fig. 3b), $\text{N}_{50\%}$ and N_B samples were consistently stable in the first 2 h (gradual settling process < 10%), showing a good kinetic stability for practical purposes. $\text{N}_{50\%}^*$ presented a rapid settling in the first 5 minutes but the KS parameters remained then stable, similarly to the other samples.

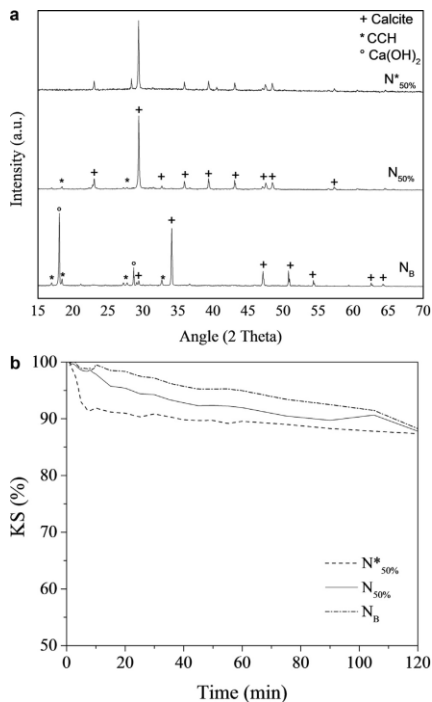


Figure 3 Analysis of the N_B , $\text{N}_{50\%}$ and $\text{N}_{50\%}^*$ suspensions, used for the treatments: a: the carbonation process in ambient air ($\text{Ca}(\text{OH})_2$, ICSD #96-100-8782; Calcite, ICSD #98-015-8258; CCH: calcium carbonate hydroxide hydrate, ICDD # 00-023-0107); **b:** kinetic stability (KS) versus time, (at $\lambda = 600 \text{ nm}$).

From the stereomicroscope investigations, the studied stones are rocks of clastic sedimentary origin composed mainly of bioclasts and whole skeletal fossil remains of marine aquatic organisms. The observed bioclasts and whole skeletal fossil remains belonged to marine bivalves, gastropods, rhodoliths, echinoderms and bryozoans. Carbonate lithoclasts were also observed together with few quartz grains. All grains were bound together by a fine-grained calcite (micrite). Based on these results, the stone samples can be classified as calcarenite, biomicrite or grainstone [41–43], commonly defined as biocalcarene and belonging to the limestone rock deposits described as “Formazione di Agrigento” [44]. The chemical analysis of the considered stone was reported in Table 1.

Table 1 XRF of the biocalcarene sample (wt %).

Ca	Si	Fe	Mg	Al	K	P
23.30	7.20	1.67	0.40	0.34	0.14	0.11

From XRD results (Fig. 4a), the main mineralogical phases were 88.8% of magnesium calcite ($\text{Mg}_{0.03}\text{Ca}_{0.97}(\text{CO}_3)$, ICSD# 980086161), 9.9% of quartz (SiO_2 , ICSD# 980083849), 1.3% of lipscombite ($\text{Fe}_{2.95}(\text{PO}_4)_2(\text{OH})_2$, ICSD# 980202937). XRD results were confirmed by FTIR investigation (Fig. 4b). The absorbance bands at 712, 876, 1429 cm^{-1} , assigned to the calcite, was readily detectable. For quartz, the absorbance bands at 798 and 1079 cm^{-1} can be attributed to absorbance of the SiO group. The peaks for goethite at 796, 912 and 1044 cm^{-1} cannot be easily distinguished due to the low concentration and the shifting with Si-O and carbonate groups. In agreement with literature results, which assessed porosity in the range 20–30% for the biocalcarene of Agrigento’s Temples [36], from MIP we obtained an average porosity of 26.1% and a density of 1.8807 g/cm^3 . In Fig. 4c the pore size distribution from MIP, referred to the three samples, is reported.

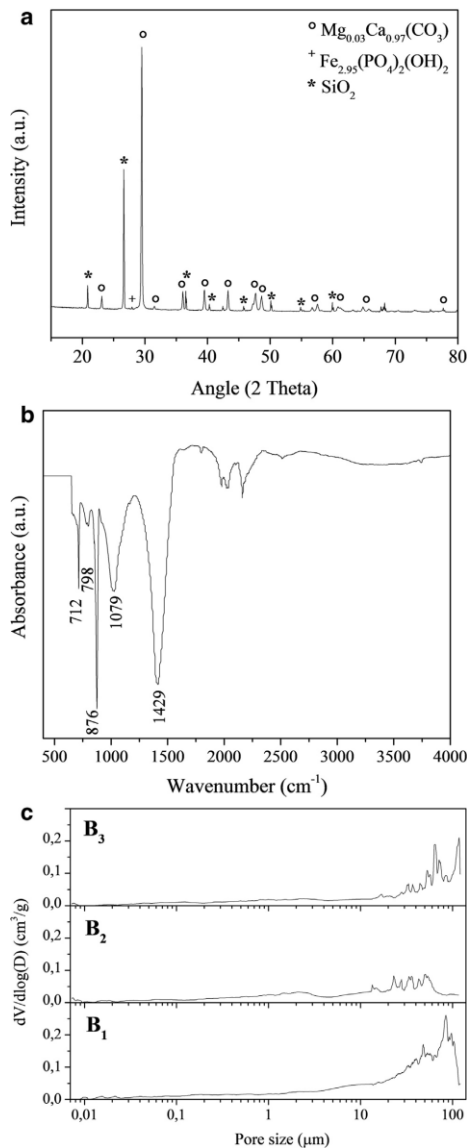


Figure 4 a–b: XRD and FTIR spectra of the biocalcarene sample; c: pore size distribution (MIP) obtained from three samples, 8 × 8 × 8 mm each.

Even if the samples presented some differences between them, the pore diameters were found to be mainly distributed in the 10–100 μm range (i.e., within the larger capillary pores range that has high capillary suction), without relevant contributions under 1 μm [45,46]. This explains the fast absorption observed below (WAC analyses) for the untreated samples as compared to the treated ones, where the larger pores have been reduced significantly. As concerns standard WAC measurements on the cubic samples, mean values of $CA = 12.7 \text{ mgcm}^{-2}\text{s}^{-1/2}$ and $Q_t = 509 \text{ mgcm}^{-2}$ were evaluated. Finally, results coming from DRMS showed values of resistance that reach 6 N within the first 3 mm, reaching a maximum value of about 10 N between 3 and 10 mm, similar to what observed from literature [47]. MIP measurements of the S1, S2 and S3 treated samples, compared to the untreated ones, are reported in Fig. 5. As concerns S1 sample (Fig. 5a), the treatment yielded an increase in the population of pores with diameters between 13 and 50 μm , and a decrease in the population of pores with diameters between 2–3 and 13 μm ; moreover, we observed a disappearing of the smallest pores ($\leq 0,1 \mu\text{m}$). In the S2 and S2 samples (Fig. 5 b–c), the treatment worked mainly to reduce the number of pores with diameters between 30–100 μm .

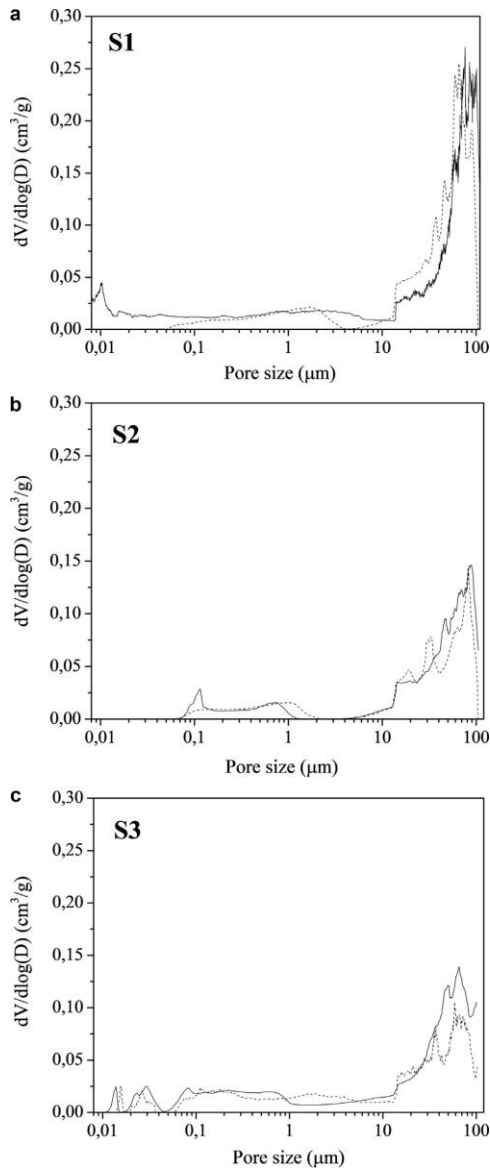


Figure 5 Differential volume of intruded mercury versus pore diameter of treated (dot lines) and untreated (continuous lines) stone samples: S1 (a), S2 (b), S3 (c).

Table 2 showed the results from the nanolime treatment on the irregular samples (WAC measurements), while in Fig. 6, we reported the WAC curves obtained for S4 and S5 before and after the nanolime treatment. It can be observed that, already after one treatment, all the samples showed a clear reduction both in the kinetics of capillary absorption (ΔCA) and in the protective efficacy E_p . In particular, we observed that the S1 sample showed the highest ability to absorb water both kinetically and in the saturation values, probably due to the higher porosity mainly related to the pores in the 10–100 μm range (Fig. 5a). In this case, the nanolime treatment seemed to have a greater influence on ΔCA than on E_p , and this could be due to the nanolime ability to reduce pore sizes by partially filling them, but without occluding them. In parallel, the samples treated by using $N_{50\%}^*$ and N_B reached the highest efficacy (about 50%) in the protection towards water. Then, when the $N_{50\%}^*$ treatment was repeated three times, the WAC results tended to improve respect to what obtained after only one treatment (Fig. 6). This

improvement was confirmed by MIP measurements, revealing a clear reduction in the population of pores with diameters between 40 and 100 μm , together with a decrease in the average porosity of about 60% (Fig. 6c).

Table 2 WAC results performed on irregular stones, before and after one nanolime treatment.

	Untreated (UT)	Treated (T)		
	Qf (mg cm^{-2})	Qf (mg cm^{-2})	ΔCA (%)	E_p (%)
S1	1013	720	44	28
S2	646	355	21	45
S3	625	324	30	48

S1, S2 and S3 were treated with $N_{50\%}$, $N^*_{50\%}$ and N_B respectively.

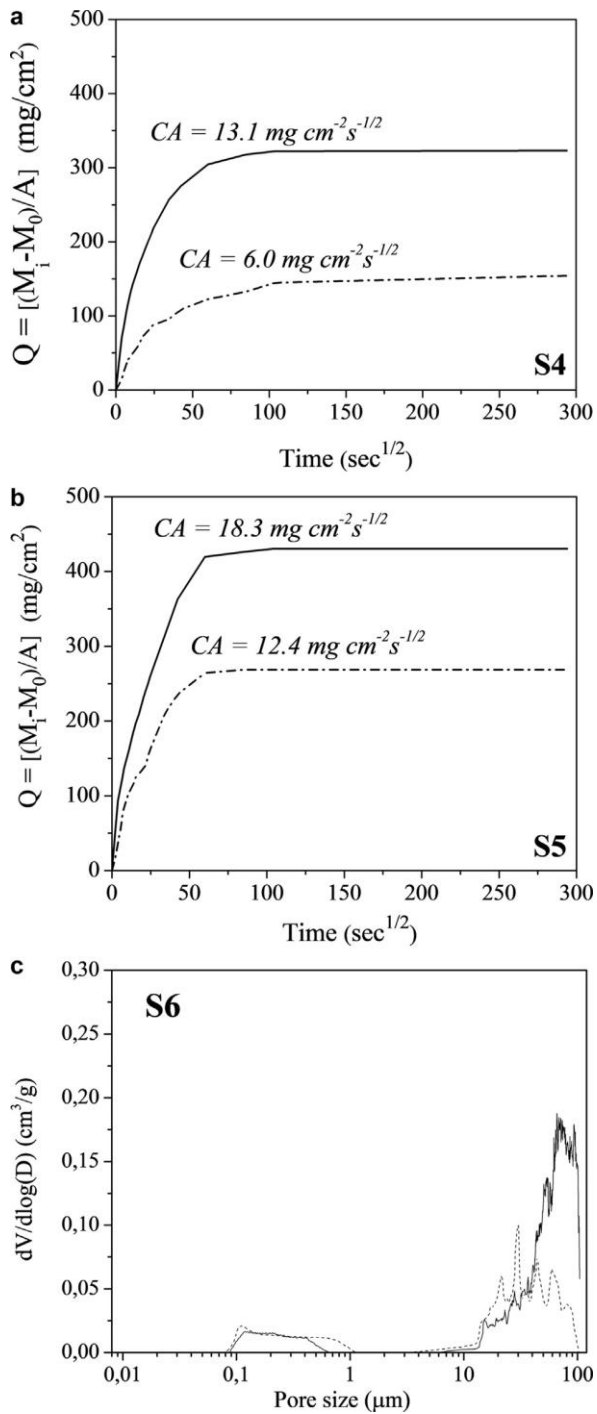


Figure 6 WAC curves and MIP measurements before (continuous lines) and after (dot lines) the $N^*_{50\%}$ treatment, repeated 3 times. CA values were reported too.

In Table 3, the STT results indicated that the nanolime treatments determined an increase of the superficial cohesion of the treated stones, with a reduction in the percentage quantity of removed material (ΔM) after one treatment of 10%, 14% and 30% for S1, S2 and S3 samples respectively. By repeating the treatment three times (S6) a clear ΔM improvement was obtained, reaching a mean value $\Delta M \approx 60\%$. The drilling resistance profiles, performed before and after the nanolime treatment, showed that a significant increase can be observed only when the treatment was repeated for three times (S6 sample). The results, reported in Fig. 7, showed that before the treatment the S6 sample presented a value of resistance of 4 ± 1 N, slightly decreasing inside the stone. After treatment, in addition to a small improvement at the surface, we observed an increase of the resistance up to 10 mm from the surface with a medium value of 8 ± 3 N. The colorimetry results were reported in Table 4, showed that the nanolime treatments do not cause major aesthetic changes (ΔE^* 5–9) and do not cause a significant increase in luminosity (ΔL^* 1–5). In particular no significant white glazing was observed after the treatment for S1, S2 and S3 (ΔL^* 3, 5 and 1 respectively). S2 seemed to show the lowest chromatic alteration of the surface (ΔE^* 5) but the highest difference of luminosity (ΔL^* 5). S3 shows higher value with $\Delta E > 9$ due to a significant alteration with $b^* > 8$ (blue-yellow axis). S2 increases the L^* parameter, probably due to the effect of higher concentration (10 g/L). The negligible chromatic changes for S1 and S2 (and ΔE^* 5–6) and the absence of a significant white glazing (ΔL^* 3–5) [40,48–50], make such nanolimes dispersions suitable for practical conservation interventions.

Table 3 Results of the STT performed on untreated and treated stones.

	UT (mg cm^{-2})	T (mg cm^{-2})	ΔM (%)
S1	1.92	1.69	9.5
S2	3.15	2.65	14.3
S3	1.17	0.57	29.6
S6	10.25	4.05	60.5

Scotch area: 12.72 cm^2 (S1, S2 and S3) and 9.5 cm^2 (S6).

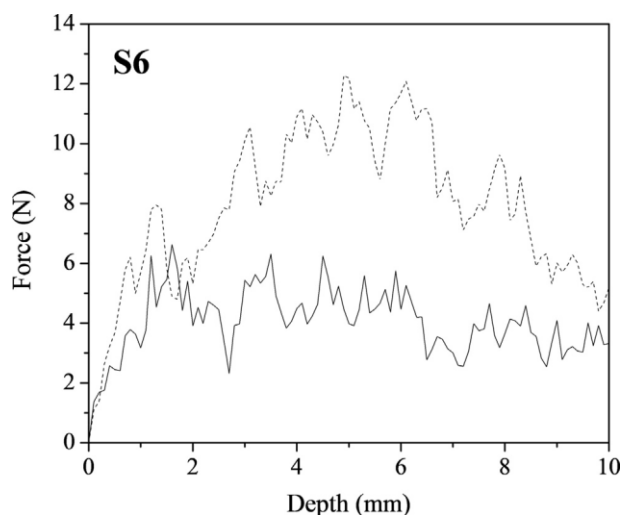


Figure 7 Drilling resistance profiles of untreated (continuous line) and treated (dotted line) biocalcarenite (S6 sample).

Table 4 Results of the colorimetric analysis performed on the treated stones.

	ΔL	Δa	Δb	ΔE
S1	3.041	-0.526	-5.170	6.024
S2	5.050	0.397	-0.003	5.065
S3	1.641	4.017	8.752	9.769

5. Conclusions

The present paper presented preliminary investigations to test the efficacy of a compatible conservative treatment for the biocalcarenite stones of the Valle dei Templi (Agrigento, Italy). The treated stone is a biocalcarenite mainly composed by calcite, with less amount of quartz, lipsocombite, and shells; the measured average porosity is about 26%, mainly distributed in the range 10–100 μm , which can be responsible for the quick water ingress by capillarity. The conservative treatments were carried out by using a nanolime, ad hoc synthesized by means of an innovative method that can guarantee high yields and a high reactivity of the final product. The characterization analyses confirmed the high reactivity of the $\text{Ca}(\text{OH})_2$ nanoparticles, reflecting a full carbonation process occurring, in ambient condition, in only the first 30 minutes. Moreover, the process led to the formation of calcite, as pure and unique phase, and this result is fundamental to guarantee a perfect compatibility with the treated surface, from a chemico-physical and mechanical point of view. As concerned the treatment efficacy, the best results were obtained by using the hydro-alcoholic nanolime suspension (50% water and 50% alcohol) at a concentration of 10 g/L, and by repeating the application for three times. This nanolime worked well as a superficial consolidant, increasing the

superficial cohesion, with a reduction of material removed from the surface up to 60%, and a good increase of the mechanical resistance particularly in the first 10 mm beneath the surface. A decrease of the water adsorption by capillarity up to 50% was observed too, confirmed by a reduced porosity and a clear reduction in the population of pores with diameters between 40 and 100 μm . Nevertheless, the nanolime treatment caused some superficial whitening that needs to be removed by proper actions or examined in depth in a next study.

Acknowledgements

The authors wish to thank Orazio Spadaro (Spadarocalce1886srl), arch. Carmelo Bennardo (Parco Archeologico Valle dei Templidi Agrigento) and Angelo Sciumè for the sampling of the materials coming from Villaseta quarry, Agrigento.

References

- [1] E. Doehne, C.A. Price, Stone conservation: an overview of current research, Second ed., The Getty conservation institute, Getty publications, Los Angeles, 2011, pp. 35–37 (Research in conservation).
- [2] F. Jroundi, et al., Bioconservation of deteriorated monumental calcarenite stone and identification of bacteria with carbonatogenic activity, *Microb. Ecol.* 60(2010) 39–54.
- [3] M. Tortora, et al., Non-destructive and micro-invasive testing techniques for characterizing materials, structures and restoration problems of mural paintings, *Appl. Surf. Sci.* 387 (2016) 971–985.
- [4] D. Costa, J. Delgado Rodrigues, Consolidation of a porous stone with nanolime, 12th Int. Congress on Deterioration and Conservation of Stone, New York (USA), 2012.
- [5] P. Baglioni, et al., Commercial $\text{Ca}(\text{OH})_2$ nanoparticles for the consolidation of immovable works of art, *Appl. Phys. A* 114 (2014) 723–732.
- [6] M.C. Mascolo, et al., An approach for a rapid determination of the aging time of lime putty, *Thermochimica Acta* 648 (2017) 75–78. [7] A. Zornoza-Indart, et al., Consolidation of a Tunisian bioclastic calcarenite: from conventional ethyl silicate products to nanostructured and nanoparticle based consolidants, *Construct. Build. Mater.* 116 (2016) 188–202.
- [8] I. Brajer, N. Kalsbeek, Limewater absorption and calcite crystal formation on a limewater-impregnated secco wall-painting, *Stud. Conserv.* 44 (3) (1999) 145–156.
- [9] A. Daehne, C. Herm, Calcium hydroxide nanosols for the consolidation of porous building materials, *EU-STONECORE, Herit. Sci.* 1 (2013) 11.
- [10] V. Daniele, et al., Synthesis of $\text{Ca}(\text{OH})_2$ nanoparticles with the addition of TritonX-100. Protective treatments on natural stones: preliminary results, *J. Cult. Herit.* 13 (2012) 40–46.
- [11] C. Rodriguez-Navarro, et al., Alcohol dispersions of calcium hydroxide nanoparticles for stone conservation, *Langmuir* 29 (2013) 11457–11470.
- [12] J. Otero, et al., An overview of nanolime as a consolidation method for calcareous substrates, *Ge-Conservación* 1 (11) (2017) 71–78.
- [13] I. Natalia, et al., Consolidation and protection by nanolime: recent advances for the conservation of the graffiti, Carceri dello Steri Palermo and of the 18th century lunettes, SS. Giuda e Simone Cloister, Corniola (Empoli), *J. Cult. Herit.* 15 (2014) 151–158.
- [14] G. Taglieri, et al., Eco-compatible protective treatments on an Italian historic mortar (XIV century), *J. Cult. Herit.* 25 (2017) 135–141.
- [15] V. Daniele, G. Taglieri, $\text{Ca}(\text{OH})_2$ nanoparticle characterization: microscopic investigation of their application on natural stones, *WIT Trans. Eng. Sci.* 72(2011) 55–66.
- [16] Z. Slizkova, et al., Consolidation of a porous limestone with nanolime, proceedings of the 12th international congress on the deterioration and conservation of stone, New York, 2012.
- [17] A. Arizzi, et al., Lime mortar consolidation with nanostructured calcium hydroxide dispersions: the efficacy of different consolidating products for heritage conservation, *Eur. J. Miner.* 27 (3) (2013) 311–323.
- [18] M. Drdác'ý, et al., A Nano approach to consolidation of degraded historic lime mortars, *J. Nano Res.* 8 (2009) 13–22.
- [19] V. Daniele, G. Taglieri, Nanolime suspensions applied on natural lithotypes: the influence of concentration and residual water content on carbonatation process and on treatment effectiveness, *J. Cult. Herit.* 11 (2010) 102–106.

- [20] G. Borsoi, et al., Understanding the transport of nanolime consolidants within Maastricht limestone, *J. Cult. Herit.* 18 (2016) 242–249.
- [21] P. Lopez-Arce, et al., Influence of relative humidity on the carbonation of calcium hydroxide nanoparticles and the formation of calcium carbonate poly-morphs, *Powder Technol* 205 (2011) 263–269.
- [22] C. Rodriguez-Navarro, et al., Kinetics and mechanism of calcium hydroxide conversion into calcium alkoxides: implications in heritage conservation using nanolimes, *Langmuir* 32 (20) (2016) 5183–5194.
- [23] B. Salvadori, L. Dei, Synthesis of Ca(OH)₂ Nanoparticles from Diol, *Langmuir* 17(2001) 2371–2374.
- [24] A. Samanta, et al., Synthesis of calcium hydroxide in aqueous medium, *J. Am. Ceram. Soc.* 99 (3) (2016) 787–795.
- [25] G. Poggi, et al., Calcium hydroxide nanoparticles from solvothermal reaction for the deacidification of degraded waterlogged wood, *J. Colloid Interface Sci.* 473 (2016) 1–8.
- [26] T. Liu, et al., Synthesis and characterization of calcium hydroxide nanoparticles by hydrogen plasma-metal reaction method, *Mater. Lett.* 64 (2010) 2575–2577.
- [27] R. Volpe, et al., A process for the synthesis of Ca(OH)₂ nanoparticles by means of ionic exchange resin, 2016 (European patent EP2880101).
- [28] G. Taglieri, et al., Analysis of the carbonation process of nanosized Ca(OH)₂ particles synthesized by exchange ion process, proceedings of the institution of mechanical engineers, Part N, *J. Nanoengineering Nanosystems* 230 (1) (2016) 25–31.
- [29] G. Taglieri, et al., Nano Ca(OH)₂ synthesis using a cost-effective and innovative method: reactivity study, *J. Am. Ceram. Soc.* 100 (2017) 5766–5778.
- [30] J. Otero, V. Starinieri, Development of a high performance nanolime for the consolidation of heritage, materials and engineering research institute doctoral research RF2 assessment, Sheffield Hallam University, 2016.
- [31] G. Taglieri, et al., Mg(OH)₂ nanoparticles produced at room temperature by an innovative, facile and scalable synthesis route, *J. Nanoparticles Res.* 17 (2015) 411–424.
- [32] R. Rossi-Manaresi, A. Tucci, Pore structure and the disruptive or cementing effect of salt crystallization in various types of stone, *Stud Conserv* 36 (1) (1991) 53–58.
- [33] R. Rossi-Manaresi, Scientific investigation in relation to the conservation of stone, science and technology in the service of conservation, IIC, London, 1982, pp. 39–45.
- [34] A.E. Charola, Salts in the deterioration of porous materials: an overview, *J. Am. Inst. Conserv* 39 (3) (2000) 327–343.
- [35] R. Giorgi, et al., A new method for consolidating wall paintings based on dispersions of lime in alcohol, *Stud. Conserv.* 45 (2000) 154–161.
- [36] C. Bennardo, et al., Comparative study of different methods for gap filling applications and use of adhesive on the biocalcarene surfaces of the “Tempio della Concordia” in Agrigento, 9th Intern. Congress on deterioration and conservation of stone, Elsevier, 2000.
- [37] M. Rosario Veiga, et al., Capillary test on historic mortar samples extracted from site. Methodology and compared results, in: 13th International Brick and Block Masonry Conference, Amsterdam, July 4-7, 2004.
- [38] ASTM D3359-02: “Standard test methods for measuring adhesion by tape test”, ASTM International, 10 August, 2002.
- [39] F. Fratini, et al., A new portable system for determining the state of conservation of monumental stones, *Mater. Struc.* 39 (286) (2006) 125–132.
- [40] C.M. Grossi, et al., Colour changes in architectural limestones from pollution and cleaning, *Color Res. Appl.* 32 (2007) 320–331.
- [41] A.W. Grabau, On the classification of sedimentary rocks, *Am. Geologist* 33(1904) 228–247.
- [42] R.L. Folk, Practical petrographic classification of limestone, *Am. Assoc. Pet. Geol. Bull.* 43 (1) (1959) 1–38.
- [43] R.J. Dunham, Classification of carbonate rocks according to depositional texture. In Ham, W.E. classification of carbonate rocks, *Am. Assoc. Petroleum Geologists Mem.* 1 (1962) 108–121.

- [44] Istituto Superiore per la Protezione e la Ricerca Ambientale, Servizio Geologico d'Italia. Note Illustrative della Carta Geologica d'Italia alla scala 1:50.000, Foglio636 Agrigento.
- [45] S. Siegesmund, H. Dürrast, Physical and mechanical properties of rocks, in: S.Siegesmund, R. Snethlage (Eds.), Stone in architecture, Springer, Berlin, Heidelberg, 2014.
- [46] A.E. Charola, E. Wendler, An overview of the water-porous building materials interactions, *Restorat. Build. Monum.* 21 (2–3) (2015) 55–65.
- [47] C. Mirabelli, et al., in: Rogerio-Candelera, Lazzari, Cano (Eds.), Effective-ness of a new nanostructured consolidant on the biocalcarene from Agrigento temples valley, international congress on science and technology for the conservation of cultural heritage, science and technology for the conservation of cultural heritage, Taylor & Francis Group, London,2013.
- [48] C. Rodriguez-Navarro, et al., alcohol dispersions of calcium hydroxide nanoparticles for stone conservation, *Langmuir* 29 (2013)11457–11470.
- [49] C.M. Grossi, et al., Color changes in architectural limestones from pollution and cleaning, *Color Res. Appl.* 32 (2007) 320–331.
- [50] NORMAL 20/85: "Interventi conservativi: progettazione esecuzione e valutazione preventiva", Roma, Italy, 1985.